



# Ethylene/ $\alpha$ -olefin homo- and copolymerization using a dinuclear catalyst of nickel

Fatemeh Nokandi<sup>1</sup> · Gholam Hossein Zohuri<sup>1</sup> · Navid Ramezani<sup>1</sup> · Hossein Hasanpour<sup>1</sup> · Mahsa Kimiaghali<sup>1</sup> · Mostafa Khoshsefat<sup>2</sup>

Received: 16 November 2023 / Accepted: 5 March 2024  
© The Polymer Society, Taipei 2024

## Abstract

Considering the essence of high electron density of ligands, frameworks with high electron donating groups are important in the transition-metal catalytic systems. As benzhydrol groups have been investigated for their beneficial electronic effects, a novel homo-dinuclear Ni (II) catalyst based on benzhydrol-substituted ligand was synthesized, characterized, and used for ethylene polymerization. The catalyst was further examined and compared with its mononuclear analogue. The maximum activity for the polymerization was then obtained at molar ratio of Al/Ni: 1500/1, polymerization temperature of 15 °C and the monomer pressure of 1.5 bar within 5 min of the polymerization which was  $2.64 \times 10^6 \text{ g mol}^{-1} \text{ Ni h}^{-1}$ . Effects of cocatalyst type (e. g., modified methylalumoxane (MMAO), triisobutylaluminum (TiBA), and triethylaluminum (TEA)) in the polymerization were also investigated wherein MMAO outperformed in terms of the greatest activity. As the polymerization temperature elevated, the polyethylene (PE) microstructure changed from crystalline into amorphous form, while both of the activity of the catalyst and the Viscosity Average Molecular Weight ( $\overline{M}_v$ ) of the obtained polymer were diminished. With regard to increasing of ethylene pressure in the reactor (up to 4 bars), the  $\overline{M}_v$  increased and reached to the maximum value of  $1.44 \times 10^6 \text{ g mol}^{-1}$ . The catalyst was also active in the presence of the long-chain  $\alpha$ -olefin monomers, such as 1-hexene and 1-octene, the comonomers. The co-monomer addition decreased crystallinity of the polymer (from 25 to 15%) and led to higher branching density of the obtained copolymers.

**Keywords** Late transition metal catalyst · Dinuclear nickel catalyst · Ethylene polymerization · Steric effect · Ethylene-1-hexene copolymerization

## Introduction

One of the research studies with a long and prominent history is the conversion of cheap olefinic monomers (such as ethylene and propylene) into widely used polyolefinic materials through transition-metal complexes [1–3]. In this regard, late transition metal (LTM) catalysts have been so far incorporated into a great deal of investigations, thanks to their diversity and interesting behaviors in the structure of chelating ligands and metal centers [4, 5]. The properties

of PE produced with such catalysts also vary from highly branched polymers to linear crystalline materials. These properties depend on the catalyst structure (namely, the type of metal and ligand) and the polymerization conditions such as temperature, pressure, etc. Such effects arise due to the competition between the propagation, migration, and termination processes [6]. In this sense,  $\alpha$ -diimine-based complexes, as well-known structures proposed by Brookhart, are endowed with an excellent performance for preparation of branched PE products [7, 8]. Researchers such as Brookhart [7–9] and Drent [7, 10] have further found that branching density can be manipulated with the ligand structure of some catalysts under polymerization conditions.

In the case of  $\alpha$ -diimines, ligand backbones and substituents on N-aryl ring can be easily modified according to the required electronic and steric features. Although significant reports have been thus far presented on different substituents and backbones of diimine-based ligand complexes

✉ Gholam Hossein Zohuri  
zohuri@um.ac.ir

<sup>1</sup> Department of Chemistry, Faculty of Sciences, Ferdowsi University of Mashhad, PO Box 91775, Mashhad, Iran

<sup>2</sup> Graduate School of Advanced Science and Technology, Japan Advanced Institute of Science and Technology, 1-1 Asahidai, Nomi, Ishikawa 923-1292, Japan

with much attention to axial donating species, asymmetric structures are still scarce [11–15]. Previous studies have also shown that the orientation of bulky substituents on axial sites can suppress chain termination or transfer (e. g.,  $\beta$ -H elimination) relatively into chain propagation [3–5, 7, 16, 17].

Over the last decade, diverse ligands bearing dibenzhydryl groups have been studied and applied in the structure of LTM catalysts for olefin polymerization. In such structures, diphenyl groups are often employed instead of common alkyl ones on *o*-positions of side aryl rings. These groups can play an effective role in providing some steric effects in axial sites, and consequently improve catalyst activity, thermal stability, and degree of branching in polymers [3, 18–23].

Besides, multinuclear catalysts with their own different structures and bridges have multiplied of these properties [24–26]. Presence of the cooperative effect between the active centers has been further reported, according to the results obtained in comparison with their mononuclear comparators, such as catalytic activity, molecular weight and molecular weight distribution, selectivity, as well as comonomer enchainment, and so on [6, 23, 27–29]. In terms of multinuclearity, two fundamental factors are much more important in controlling the cooperative effect, including the distance between the centers and the bulkiness around the active centers [23, 30].

In this study, the effect of the second metal center and bulky *o*-dibenzhydryl groups were investigated on the catalyst behavior and the obtained polymer properties. Moreover, the results were compared with the corresponding mononuclear catalyst. In addition, the impact of the polymerization parameters namely, co-catalyst nature and concentration, polymerization time, temperature, ethylene pressure, and monomer type were delineated.

## Experimental study

### Materials

All the manipulations of the air- and water-sensitive compounds were conducted under an argon/nitrogen atmosphere, using the standard Schlenk techniques or operating inside on glove box. All the solvents were also purified before use. Toluene (purity: 99.9%) (Petrochemical Co., Iran) was initially treated over sodium/benzophenone, and then utilized as a solvent for ligand synthesis and polymerization media. Dichloromethane (purity: 96%) (Sigma Aldrich Chemicals, Steinheim, Germany) was kept over phosphorus pentoxide, and subsequently distilled before being used as a solvent in synthesis of the complexed. For purifying methanol (Merck Chemicals, Darmstadt, Germany), it was heated

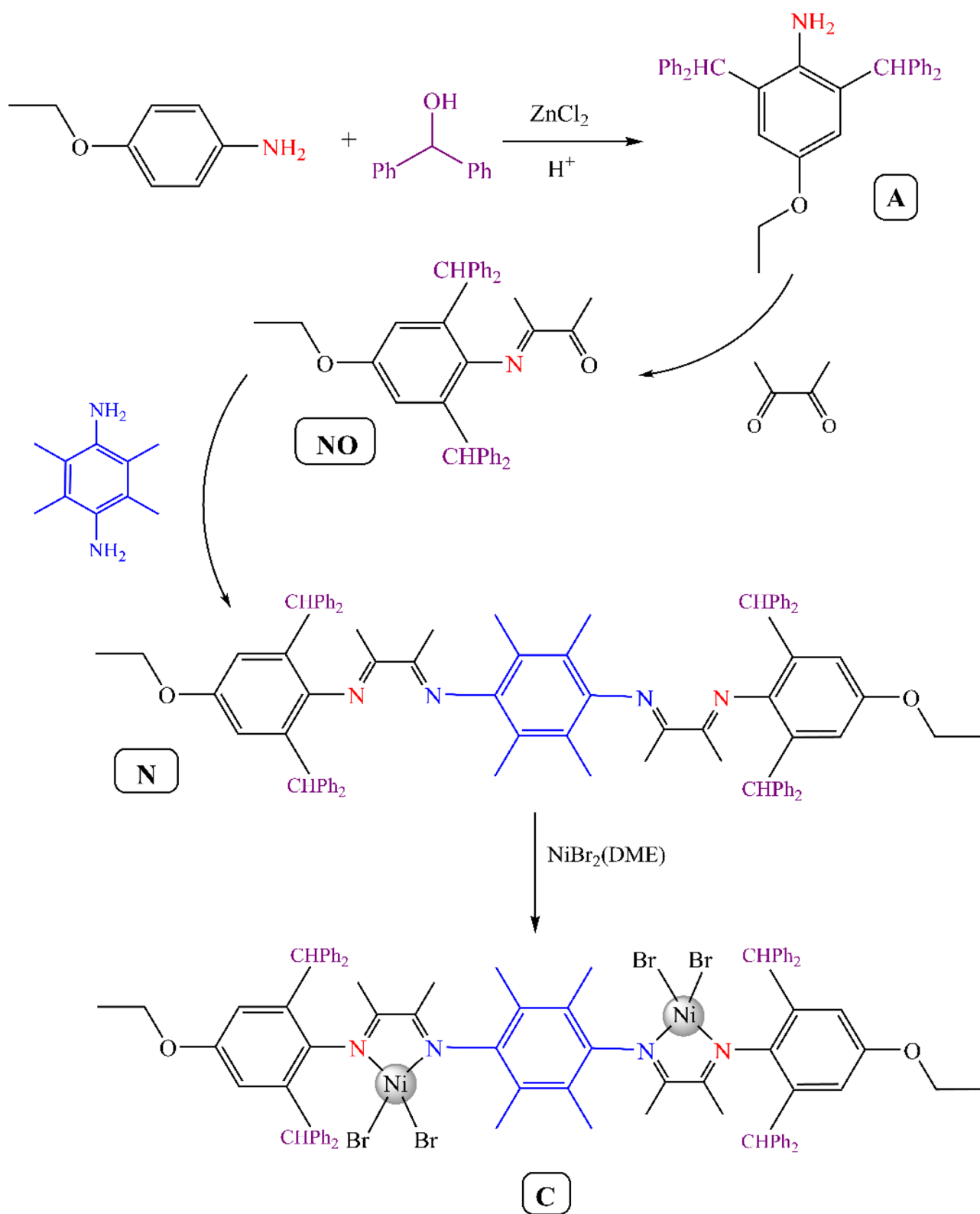
over iodine-activated magnesium with the magnesium loading of 0.5–5.0 g/L, and distilled before being applied in the synthesis of the ligand as a solvent. Polymerization-grade ethylene gas (purity: 99.9%) (Petrochemical Co., Iran) was passed through the activated silica gel, KOH, and 4Å/13X molecular sieves columns. As well, 4-ethoxy aniline (purity: 99.9%) was provided by Merck Chemicals (Darmstadt, Germany). Diacetyl (97%), diphenylmethanol (98%), 2,3,5,6-tetramethylphenyldiamine, Ni (II) bromide ethylene glycol dimethyl ether complex [(DME)NiBr<sub>2</sub>] (purity: 97%), and diethyl ether (purity: 99.5%) were similarly supplied by Merck Chemicals (Darmstadt, Germany), and used in the synthesis of the ligands and complexes. Decalin (decahydronaphthalene) (purity: 97%) was also purchased from Sigma Aldrich Chemicals (Steinheim, Germany), and utilized as a polymer solvent to determine the viscosity average molecular weight ( $\overline{M}_v$ ) of the polymer samples. Moreover, triethylaluminum (TEA, purity: 93%) and triisobutylaluminum (TiBA, purity: 93%) was supplied by Sigma Aldrich Chemicals (Steinheim, Germany), which TiBA was employed in synthesis of the modified methylaluminoxane (MMAO), as highlighted in the related literature [31]. Chlorobenzene was purchased from Sigma Aldrich Chemicals (Steinheim, Germany).

### Synthesis of ligand and corresponding complex

The final ligand (2,6-dibenzhydryl-4-ethoxy phenyl)-N = C(CH<sub>3</sub>)-C(CH<sub>3</sub>) = N- 2,3,5,6-tetramethyl benzene-N = C(CH<sub>3</sub>)-C(CH<sub>3</sub>) = N-(2,6-dibenzhydryl-4-ethoxy phenyl, Scheme 1; **N**) was prepared in two steps. Upon the preparation of the encumbered aniline (Scheme 1; **A**), the monoimine structure (Scheme 1; **NO**) was synthesized [18]. In the second step, a diamine was introduced into the monoimine compound to get the final ligand (**N**). The synthesis routes for the preparation of the ligand and the corresponding Ni complex (Scheme 1; **C**) are depicted in the Scheme 1.

### Synthesis of monoimine compound ((2,6-dibenzhydryl-4-ethoxy phenyl)-N = C(CH<sub>3</sub>)-C(CH<sub>3</sub>) = O, **NO**)

To a solution of 2,3-butadiene (1.15 mmol) and a catalytic amount of formic acid in methanol (15 ml), 2,6-dibenzhydryl-4-ethoxy aniline (**A**) (1.0 mmol) was added at room temperature. Progress of the reaction was checked using thin-layer chromatography (TLC) technique. After four days of the reaction, the solvent was evaporated under reduced pressure. The resulting powder was then dissolved in a minimum amount of hot dichloromethane. Crystallization was then formed by adding diethyl ether under low temperature. <sup>1</sup>H NMR (CDCl<sub>3</sub>, 300 MHz): 7.6–7.3 (20H, m, aryl-H), 6.6 (2H, s, aryl-H), 5.3 (2H, s, CHPh<sub>2</sub>), 3.9 (2H, q, CH<sub>2</sub>O), 2.5



**Scheme 1** The synthesis procedure of aniline (A), monoimine compound (NO), final ligand (N) and corresponding dinuclear complex (C)

(3H, s, O=C-Me), 1.4 (3H, t, CH<sub>3</sub>), 0.9 (3H, s, N=C-Me). <sup>13</sup>CNMR (CDCl<sub>3</sub>, 300MHz): 199.6 (C=O), 169.3 (C=N), 155.0 (O-CP-Ar), 142.9–114.4 (C-Aryl), 63.3 (O-CH<sub>2</sub>), 52.4 (CHPh<sub>2</sub>), 24.9 (CH<sub>3</sub>-C=O), 14.7 (CH<sub>3</sub>-C=N), 14.5 (CH<sub>3</sub>). m.p.: 150 °C. Anal. Calcd. For C<sub>38</sub>H<sub>35</sub>O<sub>2</sub>N: C, 84.15; H, 6.16; N, 2.13. Found: C, 84.88; H, 6.56; N, 2.6. FT-IR (KBr, cm<sup>-1</sup>): 1701 (–C=O), 1650 (–C=N–). Mass (EI, m/z): 537 [M+, 100%].

### Synthesis of final ligand (N)

A solution of NO (2.98 mmol), 2,3,5,6-tetramethylphenyldiamine (1.49 mmol), and *p*-toluene sulfonic acid in toluene (50 ml) was stirred at 90 °C for 24 h. The mixture was refluxed using the Dean-Stark trap for about ten days. Progress of the reaction was further checked by thin-layer chromatography (TLC) technique. <sup>1</sup>H NMR (CDCl<sub>3</sub>, 300 MHz): 7.2–7.0 (40H, m, aryl-H), 6.4 (4H, s, aryl-H), 5.2 (4H, s, CHPh<sub>2</sub>), 3.7 (4H, q, CH<sub>2</sub>O), 1.9 (12H, s, CH<sub>3</sub>Ph), 1.3–1.2 (6H, t, CH<sub>3</sub>), 0.8 (12H, s, N=C-Me). <sup>13</sup>CNMR (CDCl<sub>3</sub>, 300MHz): 170.8 (C=N), 143.3–114.4 (C-aryl), 63.3 (O-CH<sub>2</sub>), 52.4 (CHPh<sub>2</sub>), 15.9, 14.7 (CH<sub>3</sub>-C=N), 14.5 (CH<sub>3</sub>). Anal. Calcd for C<sub>86</sub>H<sub>82</sub>O<sub>2</sub>N<sub>4</sub>: C, 84.44; H, 6.82; N, 3.68. Found: C, 85.82; H, 6.87; N, 4.65. FT-IR (KBr, cm<sup>-1</sup>); the carbonyl group band (–C=O–) disappeared and the imine signal (–C=N–) intensified at 1640 cm<sup>-1</sup>.

### Synthesis of dinuclear Ni complex (C)

A mixture of (DME)NiBr<sub>2</sub> (0.17 mmol) and N (0.0831 mmol) in dichloromethane (15 mL) was stirred at room temperature under an argon atmosphere for 24 h. The solvent was then removed, and the residual solid was purified and washed with diethyl ether. FT-IR (KBr, cm<sup>-1</sup>): the imine signal was then shifted to the weak field as it coordinated to Ni; 1622 (–C=N–). Anal. Calcd. for C<sub>86</sub>H<sub>82</sub>Br<sub>4</sub>N<sub>4</sub>Ni<sub>2</sub>: C, 63.03; H, 4.86; N, 3.45. Found: C, 62.96; H, 5.04; N, 3.42.

### Polymerization

Polymerizations under low (<2 bar) and high monomer pressure were accordingly carried out in a 100 mL round-bottom flask and a 1 L Buchi bmd-300 type reactor, respectively. The round-bottom flask was also equipped with a Schlenk system, a vacuum line, an ethylene inlet, and a magnetic stirrer. The ethylene polymerization reactions, using the prepared Ni catalyst, were thus carried out under different conditions. The appropriate amount of toluene as the solvent was also introduced into the reactor under an inert atmosphere. The reactor was repeatedly evacuated and then refilled with argon and ethylene gas. After that, the co-monomer was added (in the case of copolymerization).

As well, the desired temperature was set and cocatalyst (e. g., MMAO, TiBA, or TEA) was added. The catalyst was subsequently dissolved into 2 mL of dichloromethane and introduced into the reactor. Immediately, the reactor was pressurized and the solution was stirred for specified time. The polymerization was also terminated by venting the unreacted monomer and adding 10 vol.% HCl/methanol solution. The polymer was finally washed with an excess amount of methanol and dried under reduced pressure.

### Characterization

Hydrogen nuclear magnetic resonance (<sup>1</sup>H NMR) and Fourier transform infrared (FT-IR) spectrums were initially obtained using the Bruker AC-300 and Thermo Nicolet AVATAR 370 spectrometers, respectively. Elemental analysis was also performed on the Thermo Finnigan Flash 1112EA microanalyzer. The  $\overline{M}_v$  of the polymer samples was determined according to the literature, using an Ubbelohde viscometer [32]. Intrinsic viscosity  $\eta$  was measured in decaline solvent (133 ± 1 °C) using an Ubbelohde viscometer.  $M_v$  values were calculated through Mark-Houwink [ $\eta$ ] = KM<sub>v</sub><sup>α</sup> equation (α = 0.7, K = 6.2 × 10<sup>-4</sup>). Differential scanning calorimetry (DSC) thermograms were recorded, applying the Perkin Elmer DSC Q100 instrument. The scanning electron microscopy (SEM) images were obtained by the LEO VP 1450 instrument.

## Results and discussion

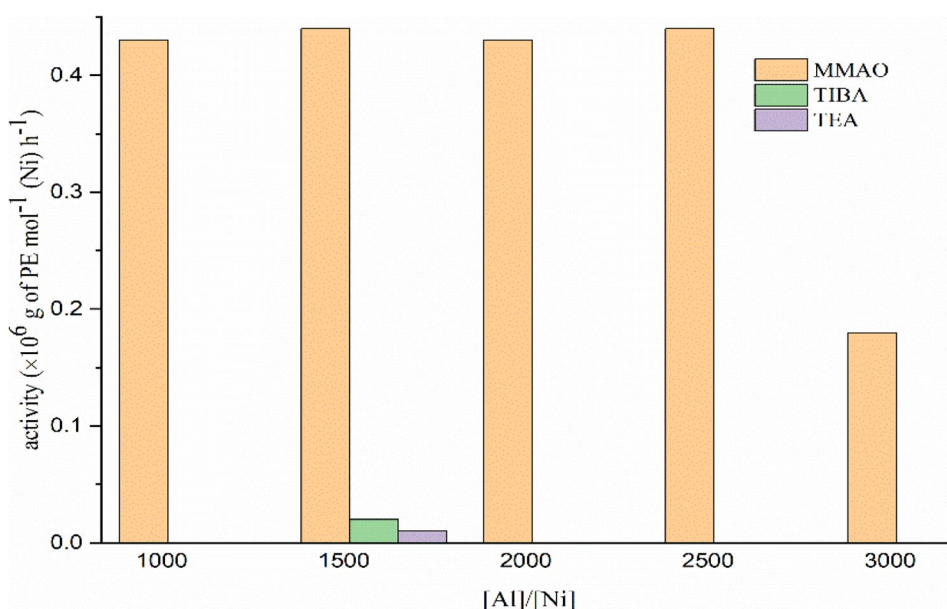
### Ethylene polymerization

To choose a good activator for the catalyst complex, three different cocatalysts were employed under similar conditions (Fig. 1). Among the cocatalysts (i. e., TiBA, TEA and MMAO), MMAO showed better ability, as a stronger Lewis acid, to activate the Ni catalyst complex as also reported [33, 34]. Accordingly, further studies were focused on the Ni/MMAO catalyst system.

The highest catalyst activity was observed at the polymerization temperature of 15 °C (1.36 × 10<sup>6</sup> g of PE mol<sup>-1</sup> (Ni) h<sup>-1</sup>) which has surpassed the same binuclear catalyst (Tables 1 and 2). The polymerization at higher temperature than 60 °C also led to a sharp drop in the catalyst activity,  $\overline{M}_v$ , and crystallinity of the polymer samples (Table 1). The highest percentage of crystallinity was also obtained at the polymerization temperature of 0 °C (i. e., 28%).

Both crystallinity and melting points dropped with increasing of the polymerization temperature (Fig. 2 and Table 1). This trend could be interpreted by some interactions and scenarios amplifying by temperature. For instance, increasing of the temperature leads to surpassing of chain transfer and

**Fig. 1** Effect of different cocatalyst on ethylene polymerization using catalyst C (Polymerization condition: polymerization time = 35 min, polymerization temperature = 25 °C, ethylene pressure = 1.5 bar, toluene = 25 ml, cat = 2.6  $\mu$  mol)



termination reactions than chain propagation. As a result, not only the length of main chain may shorten but also the probability of  $\beta$ -H elimination and reinsertion conducting branch formations could be higher. These two effect reduce the methylene sequences (thickness of lamellae) causing lower melting points and as an accumulative parameters of all segments of polymer, the crystallinity reduces [16, 25, 26, 28].

Presence of two melting points in some polymer sample implied presence of more than one active center in the catalyst. With regard to the dinuclearity of the catalyst, it

has been claimed that *syn*- and *anti*-stereoisomers are two possible isomers leading to different active site moieties ( $\Delta E_{\text{syn-anti}} = 6$  kcal/mol). The presence of *syn*- and *anti*-stereoisomers for the structures bearing a simple bond is accordingly one of the challenges facing the polymerization systems. These isomers could be thus converted once the required energy was provided [25, 33] (Fig. 3). Theoretical study (Hartree–Fock (hf) method with 6–31g\*\* basis set (by Gaussian 09W)) revealed the structure presented in Fig. 3 and Table 3.

**Table 1** The results of ethylene polymerization using catalyst C

Run	Temperature (°C)	Time (min)	Pressure (bar)	Yield (g)	Activity ( $\times 10^6$ g of PE mol <sup>-1</sup> (Ni) h <sup>-1</sup> )	$M_v^b$ ( $\times 10^4$ g mol <sup>-1</sup> )	$T_m^a$ (°C)	$X_c^a$ (%)
1	0	35	1.5	2.74	0.90	105	117,109	28
2	7	35	1.5	3.06	1.00	94	n.d. <sup>b</sup>	n.d
3	15	35	1.5	3.86	1.36	85	107, 94	25
4	25	35	1.5	1.33	0.44	24	106,55	9
5	60	35	1.5	1.21	0.40	4	20	6
6	80	35	1.5	trace	-	-	-	-
7	15	5	1.5	1.15	2.64	41	n.d	n.d
8	15	20	1.5	2.29	1.31	n.d	n.d	n.d
9	15	70	1.5	3.9	0.64	74	n.d	n.d
10	15	35	3	6.31	2.07	93	115,106	25
11	15	35	4	1.9	0.62	144	n.d	n.d

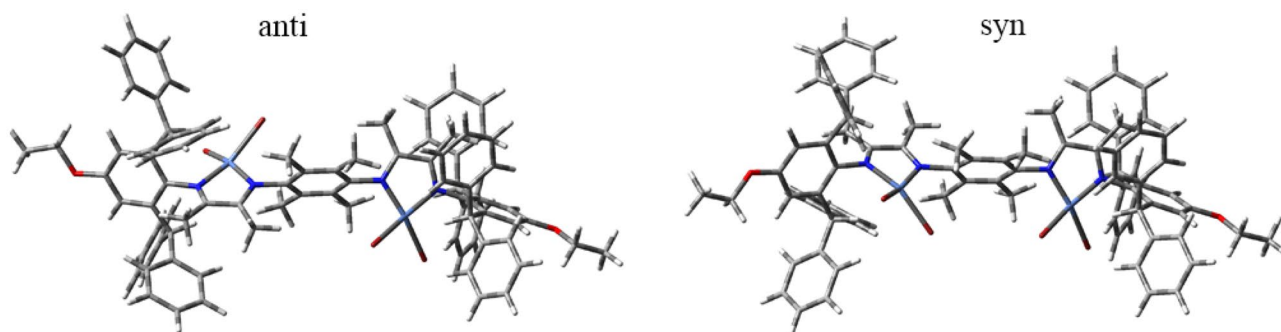
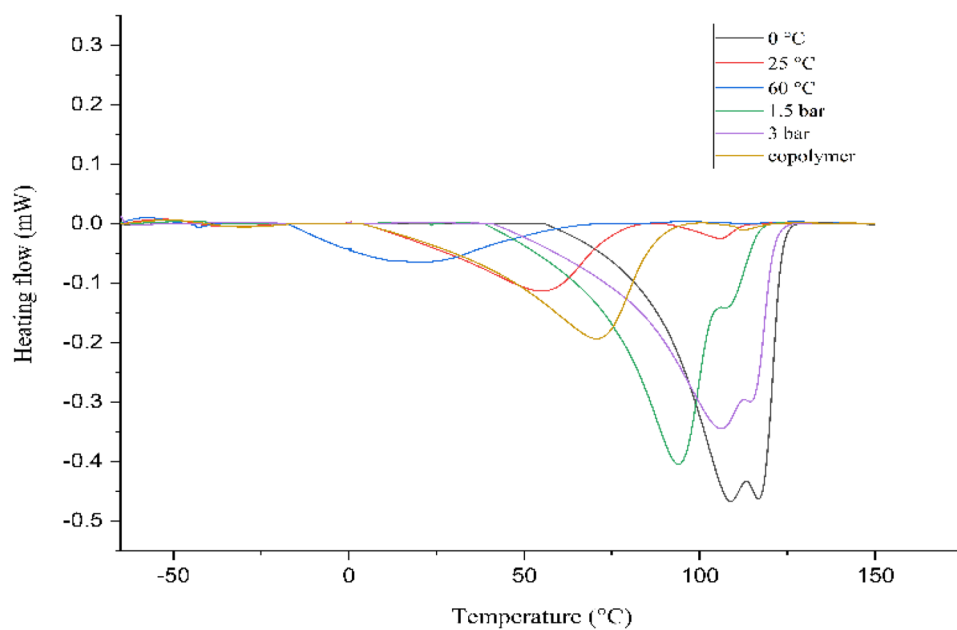
Polymerization condition: [Al]/[Ni] = 1500/1 molar ratio, toluene = 25 ml, Ni = 2.6  $\mu$ mol

<sup>a</sup>Obtained by DSC

<sup>b</sup>n. d.: not determined

**Table 2** Comparison of catalytic activity among the same binuclear catalysts

Catalyst	Activity ( $\times 10^3$ g of PE $\text{mol}^{-1}$ (Ni) $\text{h}^{-1}$ )	Reference
Synthesis of (N,N-bis(2,6-dibenzhydryl-4-ethoxy phenyl) butane-2,3-diimine) nickel dibromide	4.94	DOI: <a href="https://doi.org/10.1002/aoc.4153">https://doi.org/10.1002/aoc.4153</a>
BNC <sub>4</sub>	1.073	DOI: <a href="https://doi.org/10.1002/pola.28186">https://doi.org/10.1002/pola.28186</a>
C <sub>3</sub>	792	DOI: <a href="https://doi.org/10.1016/j.jorganchem.2005.01.029">https://doi.org/10.1016/j.jorganchem.2005.01.029</a>
{[2,6-Diisopropyl-C <sub>6</sub> H <sub>3</sub> -N=C(CH <sub>3</sub> )-(CH <sub>3</sub> )C=N-3,5-di-R-C <sub>6</sub> H <sub>2</sub> -CH <sub>2</sub> -3',5'-di-R-C <sub>6</sub> H <sub>2</sub> -N=C(CH <sub>3</sub> )-(CH <sub>3</sub> )-C=N-2,6-diisopropyl-C <sub>6</sub> H <sub>3</sub> ][NiCl <sub>2</sub> ] <sub>2</sub> ; R, -CH <sub>3</sub> }	154	DOI: <a href="https://doi.org/10.1016/j.molcata.2004.10.013">https://doi.org/10.1016/j.molcata.2004.10.013</a>
C	2640	Current study

**Fig. 2** The DSC thermograms of polyethylene (run 1, 3, 4, 5, 10) and copolymer samples made by catalyst C at different polymerization conditions**Fig. 3** The optimized stereoisomers of the catalyst C by Gaussian software

**Table 3** Selected Bond Distances (Å°), Bonding Angle (°), Dipole Moment, Mullikan Charge and Energy of the C Catalysts

Parameter	C
Ni-Br <sub>1</sub> <sup>a</sup>	2.32
Ni-Br <sub>2</sub> <sup>b</sup>	2.31
Ni-N <sub>1</sub> <sup>c</sup>	1.99
Ni-N <sub>2</sub> <sup>d</sup>	1.94
C = N	1.25
Br <sub>1</sub> -Ni-Br <sub>2</sub>	121.21
N-Ni-N	80.53
Ni-N-C (P <sub>s</sub> ) <sup>e</sup>	124.91
Ni-N-C (P <sub>i</sub> ) <sup>f</sup>	121.76
Dipole moment (Debye)	16.11
Charge of Mulliken on M	1.00
Energies (e.u.) (syn)	-16996.928
Energies (e.u.) (anti)	-16996.938

<sup>a</sup>Br1: bromine atoms in front<sup>b</sup>Br2: bromine atoms in behind<sup>c</sup>N1: nitrogen atoms connected to the side aryl ring<sup>d</sup>N2: nitrogen atoms connected to the middle aryl ring<sup>e</sup>Ps1: plane of the side aryl ring<sup>f</sup>Pi: plane of the middle aryl ring

The FT-IR analysis of the samples also confirmed their thermal properties where the integral and the intensity of the peaks at 720 cm<sup>-1</sup> (CH<sub>2</sub> sequences) and 1460 cm<sup>-1</sup> (CH<sub>2</sub> vibrations) dwindled as the polymerization temperature enhanced (Fig. 4 and Table 1). The peaks at 1380 cm<sup>-1</sup> and 1640 cm<sup>-1</sup> are related to CH<sub>3</sub> vibrations and C=C bond respectively.

SEM studies indicated that the particle morphology was well affected by the polymerization temperature (0 to 60 °C) (Fig. 5). Morphology of the particles shifted from a non-uniform island morphology to a uniform smooth and amorphous shape (Fig. 5). Moreover, the catalyst activity gradually diminished over the polymerization time of 5 to 70 min which studied. In a similar manner to the most late transition metal catalysts, the highest activity was also observed in the early stages of the polymerization (Table 1).

As polymerization time is one of the critical factors controlling the morphology of particles, the SEM images were recorded for two different periods of the polymerization. Microstructural changes, including the polymer chain growth along with the branching type and density could strongly affect the morphology of the particles. According to the FT-IR outputs, it seems that the tendency to create a polymer with lateral branches was increasing (the CH<sub>2</sub>

sequences in the peak of 720 cm<sup>-1</sup> decrease, Fig. 6) within prolong time of the polymerization. During 5 min of the polymerization, the polymer particles also demonstrated more homogeneous morphology than that in 35 min of the polymerization (Fig. 7). Another significant observation regarding the particle morphology was the growth of some fiber-like polymeric species.

Not only monomer pressure had an effect on the catalyst activity, but also the morphology and  $\overline{M}_v$  strongly affected. Upon the increase in the monomer pressure from 1.5 to 3 bars, the catalyst activity also enhanced, while, the activity decreased to 0.62 ( $\times 10^6$  g of PE mol<sup>-1</sup> (Ni) h<sup>-1</sup>) at higher pressures (i. e., 4 bars) (Table 1). The initial observations may be accordingly attributed to access of the active centers to the monomer augmentation. Later observations also indicated that the negative effect of the monomer pressure could be due to the formation of the latent sites [35].

According to the DSC thermogram, the crystallinity of the PE samples gradually and surprisingly dropped with the rising trend in the monomer pressure (Fig. 2 and Table 1). The reduction in crystallinity along with enhanced  $\overline{M}_v$  ( $1.44 \times 10^6$  g/mol) also implied the formation of the branched microstructure. This could be the result of the repetitive elimination affording macromeres and consequent reinsertions leading to LCBs. The SEM studies also revealed that the particles with completely different morphologies were produced by changing the monomer pressure (Fig. 8).

## Ethylene copolymerization

Following the positive response of the catalyst to  $\alpha$ -olefin monomers polymerization, ethylene/1-hexene and ethylene/1-octene copolymerization reactions were performed. Generally, the catalyst activity sharply decreased with the introducing of the comonomer. Upon the rising of the comonomer concentration (1-hexene), a great drop in the catalyst activity was observed toward ethylene homopolymerization (Fig. 9). The melting point and crystallinity of the copolymer were obtained to be about 71 °C and 15% respectively, at low concentration of 1-hexene. The reduction in the melting point could be attributed to the incorporation of 1-hexene comonomer into the polymer microstructure leading to thinning of lamellae thickness.

By considering the percentage of crystallinity and melting temperature (28% and 107 °C), it can be noted that the PE sample is an analogy of the low density PE (LDPE). In the presence of the comonomer, the branching density also

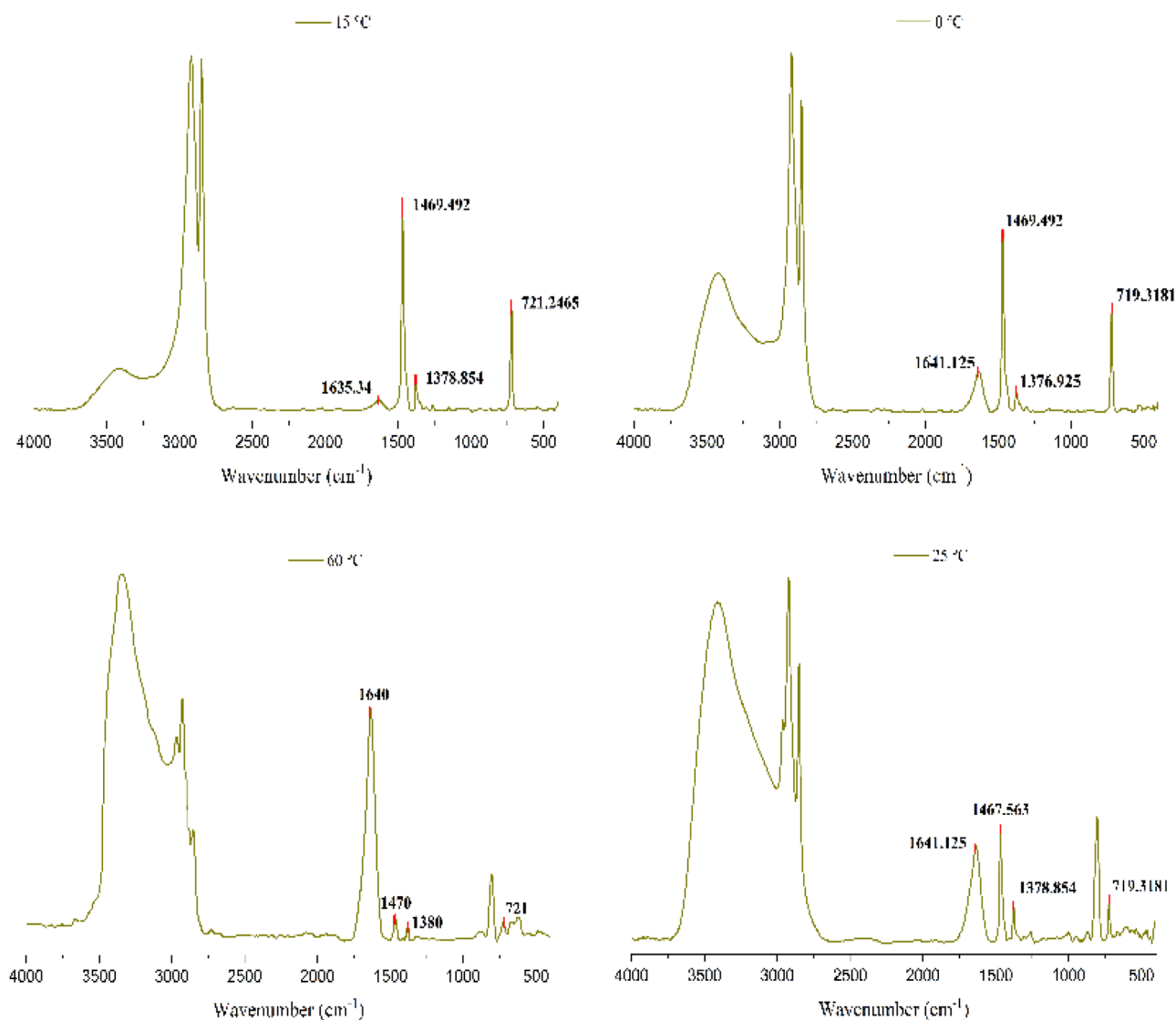
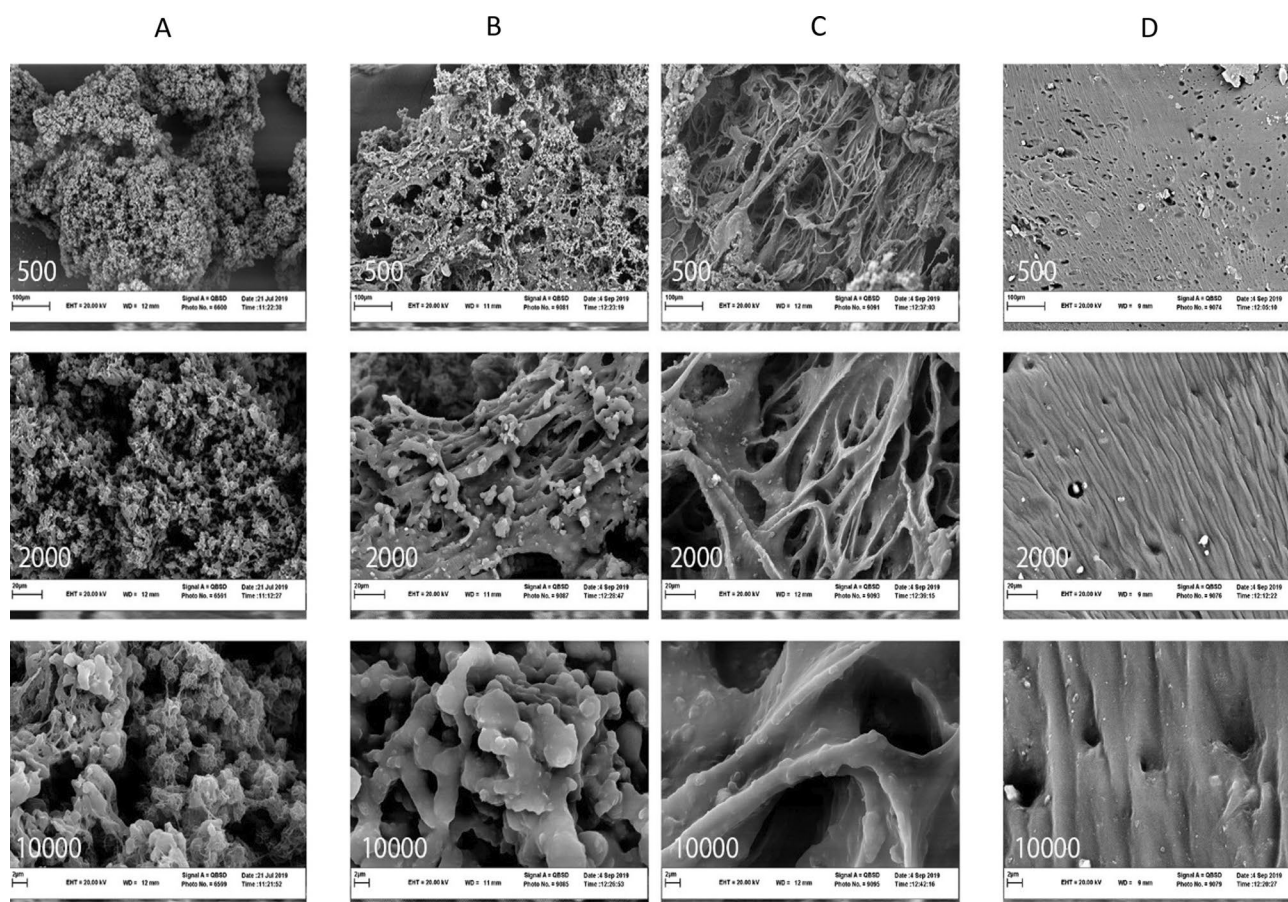


**Fig. 4** The FT-IR spectrums of PE at different polymerization temperatures using catalyst C

greatly elevated, and the final product can be assumed as the very low density PE (VLDPE) according to the results obtained from the DSC and FT-IR analyses (Fig. 10).

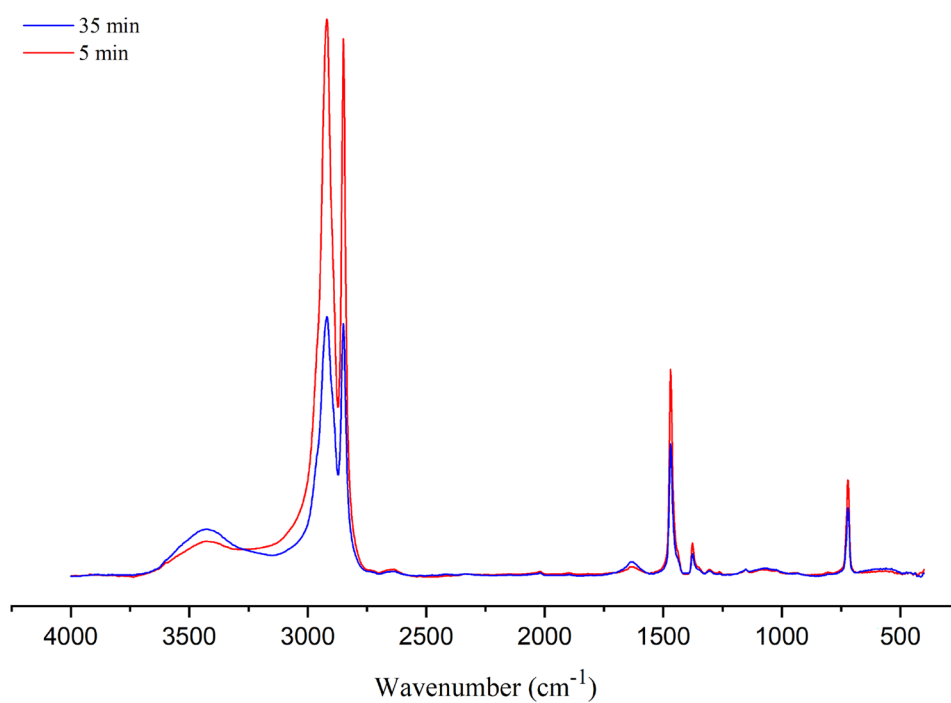
Utilizing the comonomer was also helpful in terms of polymer morphology as much more uniform shape of the particles was obtained (Fig. 11).





**Fig. 5** SEM images of PE made by catalyst C; A 0 °C, B, C 25 °C, and D 60 °C

**Fig. 6** FT-IR spectra of PE at different polymerizations time using catalyst C



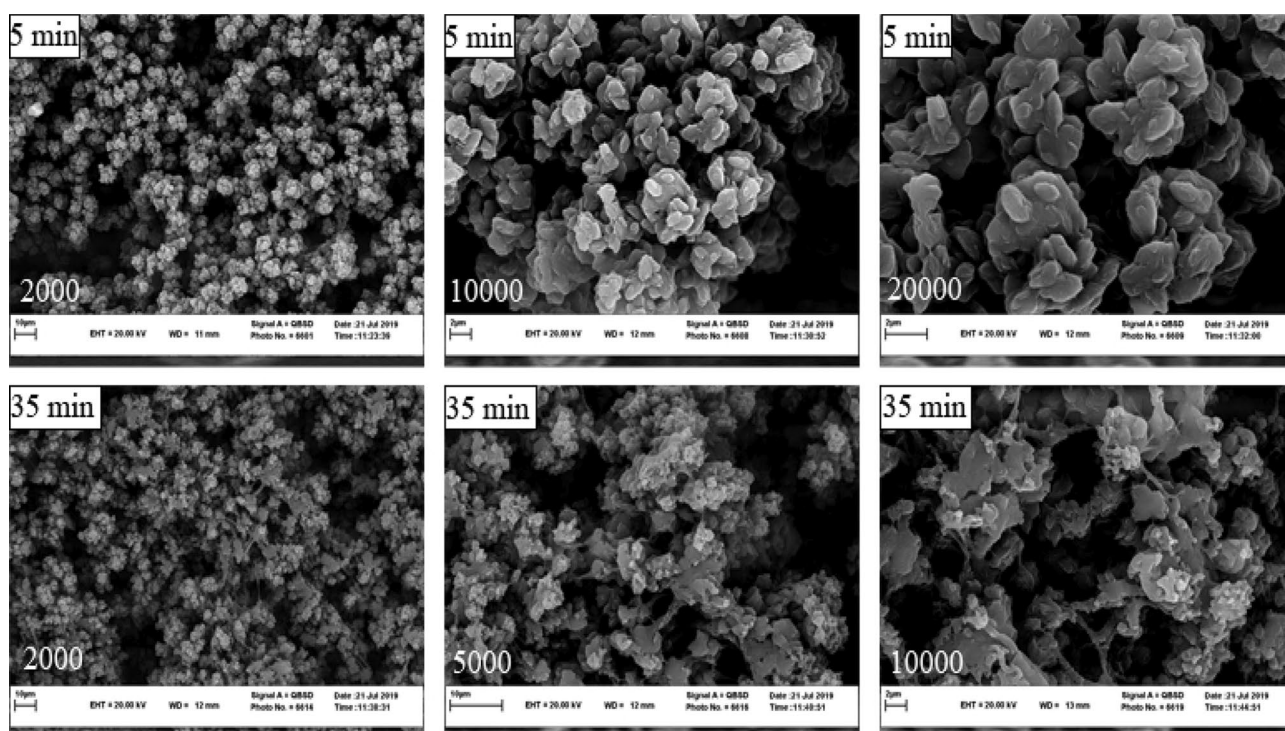


**Fig. 7** SEM images of PE made by the catalyst C at 5 and 35 min of the polymerization

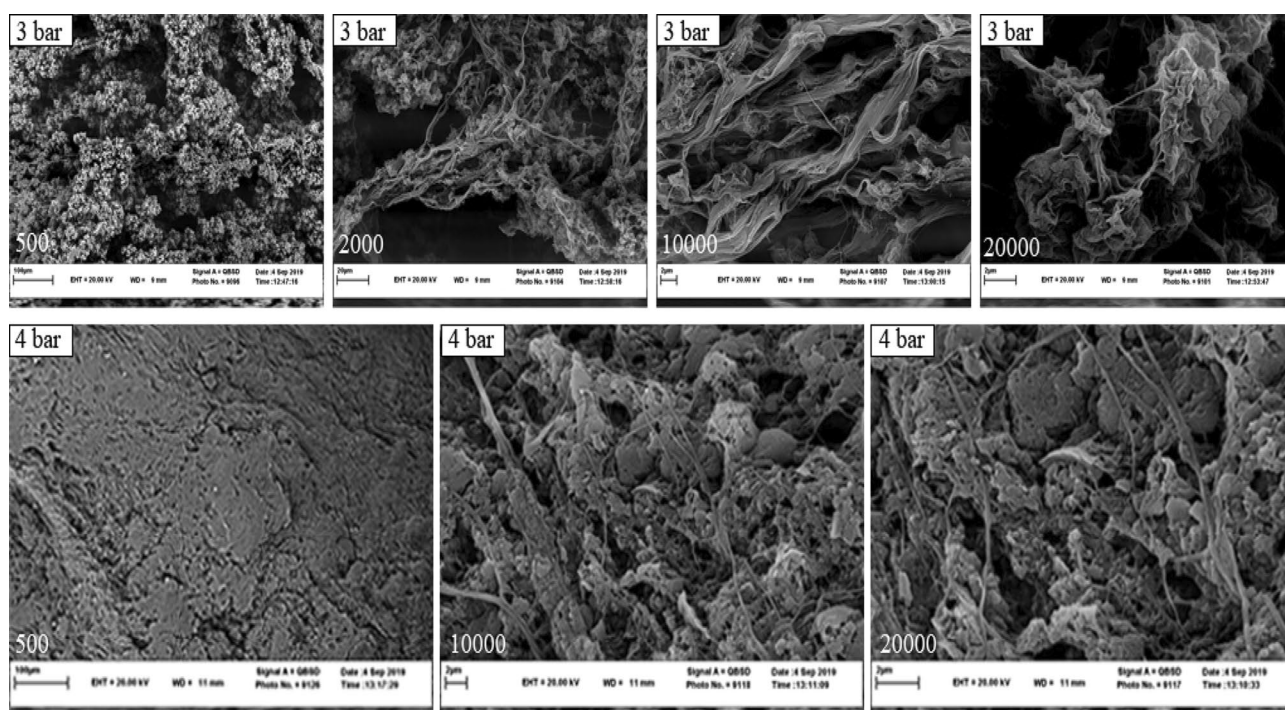


**Fig. 8** SEM images of PE made by the catalyst C at high monomer pressures

**Fig. 9** Activity of the catalyst C for ethylene homo- and copolymerization (Polymerization condition:  $[Al]/[Ni] = 1500/1$ , polymerization time = 35 min, polymerization temperature = 15 °C, ethylene pressure = 1.5 bar, toluene = 25 ml, cat = 2.6  $\mu$  mol. \*polymerization time = 24 h, room temperature. <sup>a, b</sup>Monomer concentration: 16 mmol and 63 mmol)

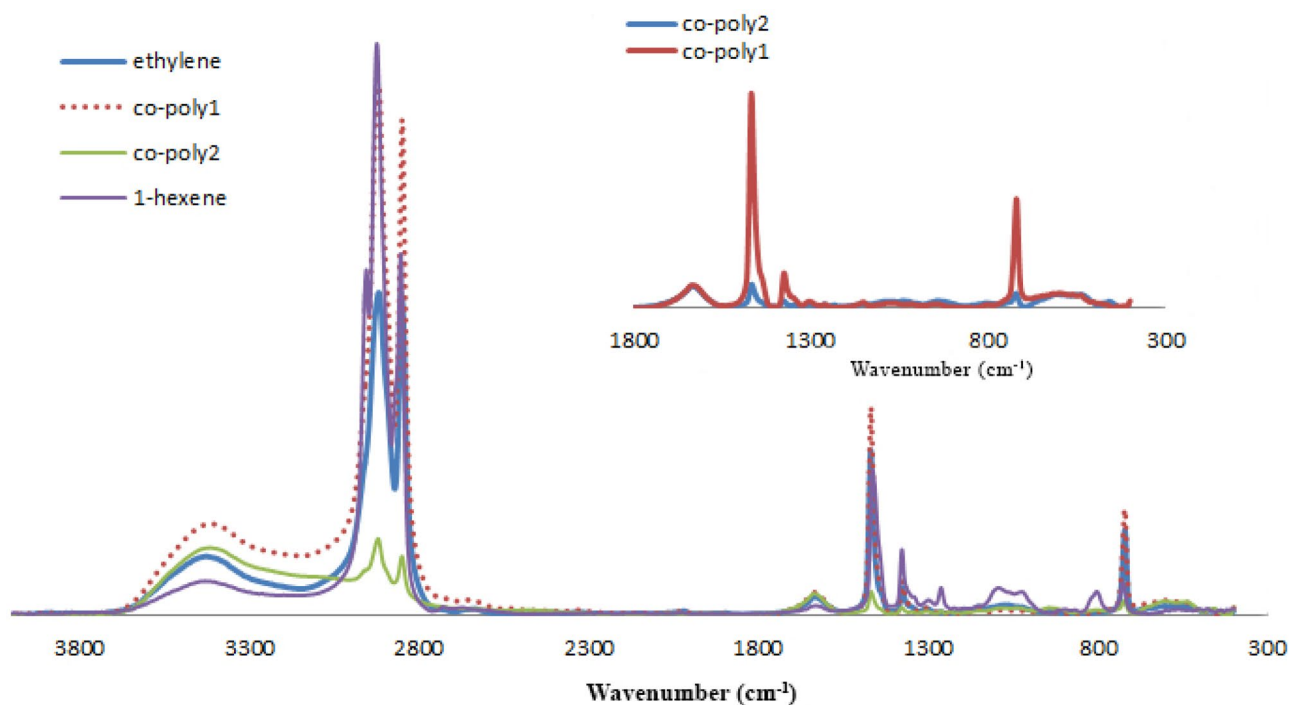
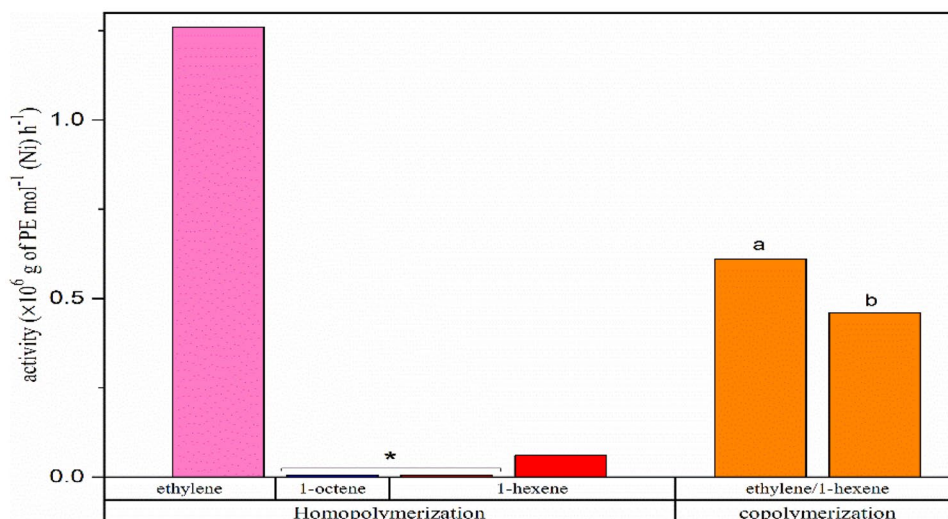


**Fig. 10** The FT-IR spectra of ethylene copolymerization using the catalyst C (co-poly1 and 2 = 16 mmol and 63 mmol concentration of the comonomer respectively)

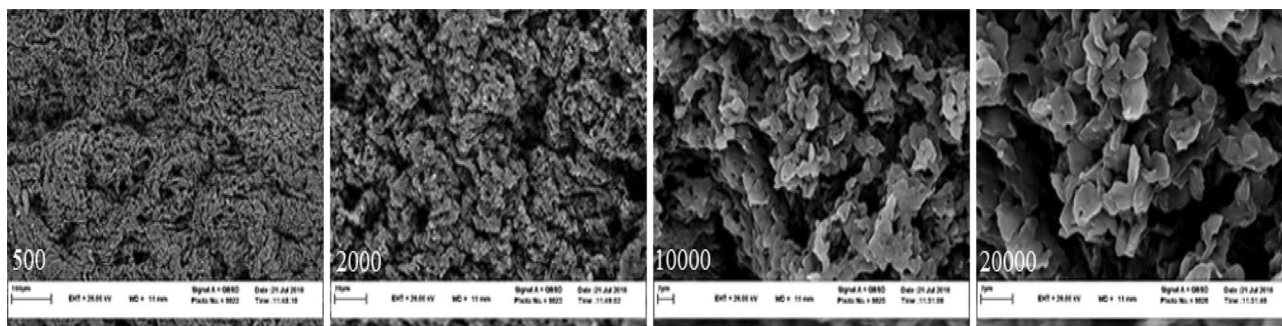


**Fig. 11** SEM images of the ethylene/1-hexene copolymer sample made using the catalyst C (see Fig. 9(b))

## Conclusion

The dinuclear catalyst bearing bulky benzhydryl groups and ethoxy substitutions showed higher activity than its mononuclear analog, which could be due to dinuclearity and optimum bulkiness around the active centers. The maximum activity of the catalyst was also obtained at 15 °C in 1.5 atm of ethylene pressure and 5 min of the polymerization in the presence of MMAO ([Al]/[Ni] = 1500/1 molar ratio) co-catalyst that was  $2.64 \times 10^6$  g PE/mol Ni. h. Considering the high electron effects of the benzhydryl and ethoxy groups in the ligand, this catalyst demonstrated relatively high activity, among other dinuclear Ni (II) based catalysts of  $\alpha$ -diimine ligand. Moreover, this catalyst activity was higher than its mononuclear counterpart, having dibenzhydryl on both *o*-positions and ethoxy on *p*-position, reported by our group. The dinuclear catalyst, unlike mononuclear analog, with very high thermal stability (up to 90 °C), was thus very sensitive to the temperature changes. Due to the presence of a bridge and the freedom of rotation around the C-N bond, the dinuclear catalysts were not active at high polymerization temperatures. As the polymerization temperature augmented, the polymer microstructural composition progressed from the crystalline to amorphous structure. Upon the increase in the monomer pressure, up to 3 bars, the activity of the catalyst amplified and reached to the maximum value.

Copolymerization of ethylene/1-hexene and ethylene/1-octene were also investigated using the dinuclear. With the increasing trend in the comonomer concentration for 1-hexene, a greater drop in the catalyst activity was consequently observed relative to the ethylene homopolymerization. The reduction in the melting point and crystallinity of the copolymer could be thus attributed to the comonomer ratio and polymer microstructure.

**Supplementary Information** The online version contains supplementary material available at <https://doi.org/10.1007/s10965-024-03944-2>.

**Acknowledgements** The authors are thankful to Ferdowsi University of Mashhad for supporting the project (FUM, project code: 3/47679).

**Author contributions** We certify that the submission is not under review at any other publications and the figures and tables in the manuscript are the original work of the authors.

**Funding** Ferdowsi University of Mashhad, 3/47679, Fatemeh Nokandi.

## Declarations

**Conflict of interest** The authors declare no conflict of interest.

## References

- Suo H, Solan GA, Maa Y, Sun WH (2018) *Coord Chem Rev*. <https://doi.org/10.1016/j.ccr.2018.06.006>
- McInnis JP, Delferro M, Marks TJ (2014) *Acc Chem Res*. <https://doi.org/10.1021/ar5001633>
- Mogheiseh M, Zohuri GH, Khoshsefat M (2018) *Macromol React Eng*. <https://doi.org/10.1002/mren.201800006>
- Khoshsefat M, Mogheiseh M, Zohuri GH, Ahmadjo S (2020) *Polym Sci Ser B*. <https://doi.org/10.1134/S1560090420330039>
- Khoshsefat M, Beheshti N, Zohuri GH, Ahmadjo S, Soleimanzadegan S (2016) *Polym Sci Ser B*. <https://doi.org/10.1134/S1560090416050067>
- Wang L, Sun J (2008) *Inorg Chim Acta*. <https://doi.org/10.1016/j.ica.2007.09.039>
- Xing Y, Wang L, Yu H, Khan A, Haq F, Zhu L (2019) *Eur Polymer J*. <https://doi.org/10.1016/j.eurpolymj.2019.109339>
- Johnson LK, Killian CM, Brookhart M (1995) *J Am Chem Soc*. <https://doi.org/10.1021/ja00128a054>
- Ittel SD, Johnson LK, Brookhart M (2000) *Chem Rev*. <https://doi.org/10.1021/cr9804644>
- Pugh RI, Drent E (2002) *Adv Synth Catal*. [https://doi.org/10.1002/1615-4169\(200209\)344:8<837::AID-ADSC837>3.0.CO;2-1](https://doi.org/10.1002/1615-4169(200209)344:8<837::AID-ADSC837>3.0.CO;2-1)
- Liu H, Zhao W, Hao X, Redshaw C, Huang W, Sun WH (2011) *Organometallics*. <https://doi.org/10.1021/om200154a>
- Mecking S (2000) *Coord Chem Rev*. [https://doi.org/10.1016/S0010-8545\(99\)00229-5](https://doi.org/10.1016/S0010-8545(99)00229-5)
- Gibson VC, Spitzmesser SK (2003) *Chem Rev*. <https://doi.org/10.1021/cr980461r>
- Wegner MM, Ott AK, Rieger B (2010) *Macromolecules*. <https://doi.org/10.1021/ma9025256>
- Popeney CS, Guan Z (2010). *Macromolecules*. <https://doi.org/10.1021/ma100220n>
- Killian CM, Johnson LK, Brookhart M (1997) *Organometallics*. <https://doi.org/10.1021/om961057q>
- Svefda SA, Brookhart M (1999) *Organometallics*. <https://doi.org/10.1021/om980736t>
- Dai S, Sui X, Chen C (2015) *Angew Chem Int*. <https://doi.org/10.1002/ange.201503708>
- Rhinehart JL, Brown LA, Long BK (2013) *J Am Chem Soc*. <https://doi.org/10.1021/ja408905t>
- Guo L, Dai S, Chen C (2016) *Polymers*. <https://doi.org/10.3390/polym8020037>
- Kimiaghahalam M, Isfahani HN, Zohuri GH, Keivanloo A (2017) *Inorg Chim Acta*. <https://doi.org/10.1016/j.ica.2017.05.005>
- Kimiaghahalam M, Isfahani HN, Zohuri GH, Keivanloo A (2018) *Appl Organomet Chem*. <https://doi.org/10.1002/aoc.4153>
- Khoshsefat M, Yanping M, Wen-Hua S (2021) *Coord Chem Rev*. <https://doi.org/10.1016/j.ccr.2021.213788>
- Khoshsefat M, Ahmadjo S, Mortazavi SMM, Zohuri GH, Soares JBP (2018) *New J Chem*. <https://doi.org/10.1039/C8NJ01678J>
- Khoshsefat M, Dechal A, Ahmadjo S, Mortazavi SMM, Zohuri GH, Soares JBP (2018) *New J Chem*. <https://doi.org/10.1039/C8NJ04481C>
- Khoshsefat M, Dechal A, Ahmadjo S, Mortazavi SMM, Zohuri GH, Soares JBP (2019) *Appl Organomet Chem*. <https://doi.org/10.1016/j.eurpolymj.2019.07.042>
- Dechal A, Khoshsefat M, Ahmadjo S, Mortazavi SMM, Zohuri GH, Abedini H (2018) *Appl Organomet Chem*. <https://doi.org/10.1002/aoc.4355>

28. Khoshsefat M, Dechal A, Ahmadjo S, Mortazavi SMM, Zohuri GH, Soares JBP (2020) ChemCatChem. <https://doi.org/10.1002/cctc.202001281>
29. Rahimpour E, Zohuri GH, Kimiaghali M, Khoshsefat M (2020) Inorg Chim Acta. <https://doi.org/10.1016/j.ica.2019.119354>
30. Wang R, Sui X, Pang W, Chen C (2016) ChemCatChem. <https://doi.org/10.1002/cctc.201501041>
31. Sangokoya SA (1996) EP Patent No 0463555:B1
32. Khoshsefat M, Zohuri GH, Ramezani N, Ahmadjo S, Haghpanah M (2016) J Polym Sci Part A: Polym Chem. <https://doi.org/10.1002/pola.28186>
33. Khoshsefat M, Dechal A, Ahmadjo S, Mortazavi SMM, Zohuri GH, Soares JBP (2019) Eur Polymer J. <https://doi.org/10.1016/j.eurpolymj.2019.07.042>
34. Jacobsen EN, Breinbauer R (2000) Science. <https://doi.org/10.1126/science.287.5452.437>
35. Kim JD, Soares JBP (2000) J Polym Sci Part A: Polym Chem. [https://doi.org/10.1002/\(SICI\)1099-0518\(20000501\)38:9%3c1427::AID-POLA4%3e3.0.CO;2-Y](https://doi.org/10.1002/(SICI)1099-0518(20000501)38:9%3c1427::AID-POLA4%3e3.0.CO;2-Y)

**Publisher's Note** Springer Nature remains neutral with regard to jurisdictional claims in published maps and institutional affiliations.

Springer Nature or its licensor (e.g. a society or other partner) holds exclusive rights to this article under a publishing agreement with the author(s) or other rightsholder(s); author self-archiving of the accepted manuscript version of this article is solely governed by the terms of such publishing agreement and applicable law.